Title

The genetic basis of divergent melanic pigmentation in benthic and limnetic threespine stickleback

Authors

Tapanes, Elizabeth

Rennison, Diana J

Publication Date

2024-07-24

DOI

10.1038/s41437-024-00706-0

The genetic basis of divergent melanic pigmentation in benthic and limnetic threespine stickleback

Elizabeth Tapanes[1], Diana J. Rennison[1]

[1]School of Biological Sciences, Section of Ecology, Behavior & Evolution, University of California San Diego, La Jolla, CA, USA

Corresponding author email: drennison@ucsd.edu

Word count for main text: 4,744

Abstract

Pigmentation is an excellent trait to examine patterns of evolutionary change because it is often under natural selection. Benthic-limnetic threespine stickleback (*Gasterosteus aculeatus*) exhibit distinct pigmentation phenotypes, likely an adaptation to occupation of divergent niches. The genetic architecture of pigmentation in vertebrates also appears to be complex. Prior QTL mapping for threespine stickleback pigmentation phenotypes has identified several candidate loci. However—relative to other morphological phenotypes (e.g., spines or lateral plates)—the genetic architecture of threespine stickleback pigmentation remains understudied. Here, we performed QTL mapping for two melanic pigmentation traits (melanophore density and lateral barring) using benthic-limnetic F_2 crosses. The two traits mapped to different chromosomes, suggesting a distinct genetic basis. The resulting QTLs were additive, but explained a relatively small fraction of the total variance (~6%). QTLs maps differed by F_1 family, suggesting variation in genetic architecture or ability to detect loci of small effect. Functional analysis identified several enriched pathways for candidate loci. Several of the resulting candidate loci for pigmentation, including three loci in enriched pathways (*bco1*, *sulf1*, and *tyms*) have been previously indicated to affect pigmentation in other vertebrates. These findings add to a growing body of evidence suggesting pigmentation is often polygenic.

Keywords: coloration, pigmentation, melanocyte, phenotypic variation, genetic architecture, fish

Introduction

Across the animal kingdom, pigmentation serves as an important communication signal (or disruptor) intra- and interspecifically and thus is often under natural and sexual selection (Cuthill et al., 2017; Hubbard et al., 2010; Orteu & Jiggins, 2020; Protas & Patel, 2008). Pigmentation and patterning are critical for many key biological functions or interactions– including mate choice, thermoregulation, microbial resistance, crypsis, toxicity warning, and mimicry (Cuthill et al., 2017; Protas & Patel, 2008). These signals are often generated through a combination of pigment cells and reflective structures, and both pigmentation and patterning are under strong genetic control (Jablonski & Chaplin, 2017; Lopes et al., 2016; Luo et al., 2021; Nachman et al., 2003). As such, animal pigmentation genetics has emerged as a robust model system to study the phenotype-genotype relationship. The interest in this trait has led to the identification of hundreds of loci and pathways involved in vertebrate pigmentation (Elkin et al., 2022; Hidalgo et al., 2022; Kelsh, 2004; Lamoreux et al., 2010). However, studies on the genetic basis of pigmentation are often biased toward certain taxonomic groups (e.g., mice, humans), populations, and/or candidate loci (e.g., *mc1r*, *agouti*) (Elkin et al., 2022; Tapanes et al. 2022)). For example, ~70% of known pigmentation candidate genes emerged from mammalian studies, but only 5% are associated with fish (Elkin et al., 2022). Additional taxa and loci must be studied and identified to gain a more comprehensive and unbiased understanding of the genetic architecture of pigmentation.

Through characterization of the genetic architecture of pigmentation we gain insight into evolutionary phenomena, including the predictability of phenotypic and genotypic evolution as well as the origins of adaptive genetic variation (Cuthill et al., 2017; Elkin et al., 2022; Martin & Orgogozo, 2013). So far, work suggests that often the same loci are co-opted across vast

66 evolutionary scales to produce convergent pigmentation phenotypes (Crawford et al., 2017;
67 Lamason et al., 2005; Miller et al., 2007; Saenko et al., 2015)). For example, *oca2* underlies
68 melanin deficiency in humans and corn snakes. Frequent identification of major effect genes
69 (e.g. *mc1r*) in studies of specific populations (i.e., mice, European people) led to the assumption
70 that pigmentation has a simple genetic architecture, with mutations of large effect generating key
71 phenotypes (Hubbard et al., 2010; Protas & Patel, 2008; Quillen et al., 2019). However, recent
72 evidence suggests the underlying genetic architecture of this trait may frequently be complex
73 (highly polygenic) (Anderson et al., 2009; Jones et al., 2018). Pigmentation can exhibit rapid
74 phenotypic and genetic change, quickly evolving within a handful of generations, adapting to
75 new environments (Barrett et al., 2019; Jones et al., 2018). To fully understand pigmentation in
76 light of evolutionary change, we must be able to robustly characterize the genetic architecture in
77 more than a handful of organisms.
78 The threespine stickleback (*Gasterosteus aculeautus*; hereafter referred to as
79 'stickleback') offers an opportunity to study key evolutionary processes and patterns, such as—
80 evolutionary predictability and adaptation and with ample genetic resources it is possible to
81 characterize genetic architecture of adaptive traits. Marine stickleback repeatedly and rapidly
82 colonized newly formed freshwater habitats at the end of the Pleistocene (≈12,000 years ago)
83 (Bell & Foster, 1994). Within lakes and streams, stickleback independently adapted to the local
84 ecological conditions–often diverging along a benthic-limnetic axis. Within a handful of lakes
85 there has been the evolution of sympatric benthic and limnetic ecotypes which utilize the littoral
86 and pelagic regions of the lakes, respectively (Schluter & McPhail, 1992). These sympatric
87 ecotypes have diverged both genetically and phenotypically in response to their divergent niches
88 (Jones et al., 2012; Peichel et al., 2001; Schluter & McPhail, 1992). Notably, phenotypic

89 divergence involves suites of trophic (Schluter & McPhail, 1992) and defensive traits (Vamosi &
90 Schluter, 2004). However, the ecotypes have also diverged in several pigmentation traits (Clarke
91 & Schluter, 2011; Greenwood et al., 2011; Gygax et al., 2018; Miller et al., 2007).
92 Limnetic fish exhibit greater ventral pigmentation (Miller et al., 2007) and more lateral
93 barring than benthic fish (Greenwood et al., 2011). Increased brightness has been associated with
94 increased use of limnetic resources (French et al., 2018; Bolnick & Ballare, 2020; Lavin &
95 McPhail, 1986). Additionally, green pigmentation in the dorsal region is more prevalent in
96 benthic fish (Clarke & Schluter, 2011; Gygax et al., 2018). Males of each ecotype also differ in
97 their nuptial coloration—limnetic males exhibit redder throat patches relative to benthic
98 stickleback, and often have an intensely blue iris (Boughman, 2001). Differences in pigmentation
99 are predicted to be adaptive as there is covariance with the spectral qualities of each ecotype's
100 primary habitat (littoral vs. pelagic) (Clarke & Schluter, 2011; Rennison et al., 2016); and the
101 preferred nest sites of the two ecotypes also differ in spectral quality (Boughman, 2001). The
102 visual sensitivities of the two ecotypes exhibit divergence (Boughman, 2001; Rennison et al.,
103 2016), suggesting differential perception of intra- and inter-specific pigment signals could
104 contribute to pigmentation divergence (Boughman, 2001). Further, there are distinct predation
105 regimes between the habitats (Vamosi & Schluter, 2004) and differential exposure to a vertebrate
106 predator has been found to be associated to divergence of pigmentation (Gygax et al., 2018),
107 suggesting selection due to crypsis may also drive the evolution of pigment differences.
108 Quantitative trait mapping (QTL) studies for some stickleback pigmentation traits have
109 successfully identified candidate genes or genomic regions. So far, work using marine-
110 freshwater pairs has characterized candidate regions for two pigmentation traits: lateral barring
111 and ventral melanism (Greenwood et al., 2011; Greenwood et al., 2012). Candidate regions have

also been found for both male and female nuptial coloration, specifically male red throat chroma was mapped in a benthic-limnetic pair (Malek et al., 2012) and red throat and pelvic spine pigmentation in females from allopatric stickleback populations (Yong et al., 2016). Yet, in general we know little about the genetic architecture of pigmentation traits of stickleback or how the genetic architecture varies across populations. More than 1,000 QTL have been identified for various stickleback phenotypes (behavioral, morphological or life history), but only 20 (1.7%) are associated with pigmentation traits. Furthermore, of the 27 threespine stickleback QTL studies included in a 2017 meta-analysis of stickleback QTL, only four studies mapped pigment traits (Peichel & Marques, 2017). Gene expression studies have been useful in identification of pigment associated genes (McKinnon et al., 2022).

Here, we conducted a QTL mapping study of two melanin-based pigmentation phenotypes—melanophore density and lateral barring using threespine stickleback benthic-limnetic F_2 crosses. We focused on these traits as there is experimental evidence that melanism and lateral barring are adaptive phenotypes, diverging in response to differential predation pressures (Gygax et al., 2018), which aids in vertebrate predator avoidance. Once candidate regions were identified, functional enrichment analyses were used to further characterize the resulting loci.

Materials and Methods

Four F_1 crosses were made in Spring of 2011 using four benthic females and four limnetic males collected from Paxton Lake on Texada Island, British Columbia, Canada. These F_1 families were reared in 100L tanks under standard laboratory conditions for nine months. Once the fish reached reproductive maturity in Spring of 2012, each F_1 family was split between a pair

of semi-natural ponds (n = 8 ponds), which were located on the University of British Columbia campus in Vancouver, Canada. The pond rearing facility and cross design have been previously described (Arnegard et al., 2014; Rennison et al., 2019). Each pond was 25m x 15m, and included a vegetated littoral zone as well as a deep-water habitat of 6m (S1). The ponds contained typical natural food resources and invertebrate predators. Once in the ponds, the F_1 fish reproduced naturally from May – July 2012. In fall of 2012, a sample of the resulting juvenile F_2 fish was taken from each pond (S2). Immediately following collection by minnow trap or net, fish were euthanized using MS-222 and preserved in 95% ethanol. The fish were fin clipped for DNA extraction and subsequent genotyping.

Pigmentation variation

We phenotyped two pigmentation traits in our F_2 sample (N = 400)—melanophore density and lateral barring (Figure 1). Using Adobe Photoshop, we estimated melanocyte density by manually counting the number of visible melanocytes on the fin junction using the 'count tool' and dividing the resulting count value by the total area (in mm) (*similar to* (Miller et al., 2007)) (S3). We estimated lateral barring by converting each photo to black and white and estimating the absolute difference between a light and dark patch on the ventral flank (S4). This was done by selecting two squares 11x11 pixels in size, and placing the first point on the dark bar superior to the start of the anal fin. If the fish exhibited a clear barring pattern, the second square was placed on the brighter region between the two dark bars. If the fish lacked a clear barring pattern, we selected two squares at an average distance typical of two dark bars (≈1.12mm) and took the absolute difference between both points. To account for potential differences in lighting conditions across each photo, we divided the absolute difference by the

158 average grey value of the photo, and then multiplied that number by 100 (*similar to* (Greenwood
159 et al., 2011)).
160 Since some previous pigmentation work has relied on scoring phenotypes on living fish
161 (Greenwood et al., 2011; Gygax et al., 2018; Clarke & Schluter, 2011), we first sought to test the
162 validity of scoring melanic pigmentation on stained and preserved fish. Our verification sample
163 included live wild marine (Sooke, Courtenay, Sayward estuaries) and freshwater (Mohun,
164 Comox, and Muchalat lakes) populations (N= 170) that were collected in British Columbia in
165 Spring 2021. We photographed fish prior to euthanasia against an X-rite color checker passport
166 using a Nikon D500 mounted with the AF-S DX NIKKOR 16-80mm f/2.8-4E ED VR lens (S5).
167 We set a manual white balance by calibrating the camera with a grey standard in the field. All
168 fish were photographed against a blue background following established protocols (Gygax et al.,
169 2018; Stevens et al., 2007). Instead of melanophore density, we scored brightness as a proxy for
170 overall pigmentation as brightness is a good measure of the relative prevalence of black
171 pigmentation. This was necessary because the melanophore density was difficult to score on
172 many of the marine individuals due to the presence of other colors (e.g., silver iridescence) and
173 bony elements. We estimated an individual's brightness using the Red-Green-Blue (RGB) color
174 model sampled from the skin at the fin junction. We scored lateral barring following the same
175 methodology used on preserved specimens (described above). Following tissue fixation in
176 formalin and alizarin red staining following the protocol of Peichel et al., 2001, the fish were re-
177 photographed and scored for melanophore density and lateral barring. A Pearson correlation test
178 was used for both traits in order to assess if there was a meaningful relationship between
179 pigmentation estimates obtained from stained versus living fish. A negative (melanophore
180 density vs brightness) or positive correlation (lateral barring) between pre and post staining

measurements (at $p < 0.05$) indicated our stained pigment measurements indeed captured a meaningful aspect of biological reality.

Experimental Crosses

The mapping fish were the product of four F_1 crosses made in the spring of 2011, between four pairs of benthic mothers and limnetic fathers collected from Paxton Lake on Texada Island, British Columbia, Canada. The F_2 fish were the product of natural mating among F_1 siblings that had been introduced into eight semi-natural experimental ponds located on the University of British Columbia Campus in Vancouver, Canada. There was one F_1 family per pond, with two ponds per family.

QTL mapping

The underlying genotype data was generated for and used in a previously described experiment (Rennison et al., 2019). DNA was extracted from each F_2 individual's fin clip (N = 400, 50 from each pond) using a standard phenol-chloroform extraction protocol. DNA was also extracted from the F_1 parents and F_0 grandparents. Libraries were prepared using the *PstI* enzyme following a genotyping by sequencing protocol (*as in* (Elshire et al., 2011)) and sequenced on an Illumina Hi-Seq 2000 platform. A standard reference based bioinformatics pipeline was used to identify sequence variants (single nucleotide polymorphisms, SNPs) (see archived code from Rennison et al., 2019 for full details). Briefly, after demutiplexing, Trimmomatic (Bolger et al., 2014) was used to filter out low quality sequences and adapter contamination. Reads were aligned to the stickleback reference genome (Jones et al., 2012) using BWA v0.7.9a (Li & Durbin 2009) with subsequent realignment using STAMPY v1.0.23 (Lunter & Goodson, 2011).

For genotyping the GATK v3.3.0 (Mckenna et al., 2010) best practices workflow (DePristo et al., 2011) was followed except that the MarkDuplicates step was omitted. RealignTargetCreator and IndelRealigner were used to realign reads around indels and HaplotypeCaller identified single nucleotide polymorphisms (SNPs) in individuals. Joint genotyping was done across all individuals using GenotypeGVCFs. The results were written to a single VCF file containing all variable sites. This file was filtered for a minimum quality score (of 20) and depth of coverage (minimum of 8 reads and maximum of 100,000) before use in downstream analyses.

A pedigree was built using the MasterBayes R package and a set of 1,799 SNPs, which had minimal (< 10%) missing data across all individuals. In order to have fully informative markers, only SNPs that were homozygous for alternative alleles in the benthic and limnetic grandparents of each F_2 cross were used. These SNPs were then used to calculate pairwise recombination frequencies and create a genetic map using JoinMap version 3.0 (Ooijen & Voorrips, 2002). In total, 398 F_2 progeny from the four F_1 crosses were used for mapping, with many F_2 families. F_2 genotypes were coded according to the population code for outbred crosses, allowing segregation of up to four alleles per locus (cross-pollinator). The JMGRP module of JoinMap was used with a LOD score threshold of 4.0 to assign 2,243 loci to 33 linkage groups. For each linkage group, a map was created with the JMMAP module. Mapping was done using the Kosambi function with a LOD threshold of 1.0, recombination threshold of 0.499, jump threshold of 5.0, and no fixed order. Two rounds of mapping were performed, with a ripple performed after each marker was added to the map.

QTL mapping was performed using Haley-Knott regressions across the F_1 families (all-family QTL) and individual sex and family were set as covariates in the R/qtl package (Broman & Sen, 2009) with 2,037 SNP markers spread across the 21 chromosomes. The marker density

was on average 4.2 SNP markers per kilobase (kb) (mean range across chromosomes 2.3 – 5.9 SNPs/kb). To test if there was any variation among the four F_1 families in the genetic basis of divergent pigmentation, we also performed QTL mapping independently for each family (within-family QTLs) with sex as a covariate, and sample sizes of 93-99 individuals per F_1 family. We calculated the percentage variance explained (PVE) for each candidate locus using the equation: PVE = 1 – (10^(-2*(LOD/n))), where LOD is the estimated LOD score and n is the sample size. The significance threshold for each phenotype was estimated using permutation testing with 10,000 iterations. Overall phenotypic heritability for the two pigmentation traits was calucated by estimating a kinship matrix using the *kinship2* R package and the *est_herit* function in the *qtl2* package.

Functional enrichment testing

We identified candidate genes from within the 1.5 LOD interval region surround the QTL peaks; the resulting candidates were then explored through comparisons to existing candidates from other taxa and using functional enrichment testing. First, we determined whether any of the candidate loci found within our QTL peaks had been previously associated with pigmentation in other vertebrates. To this end, we determined what genes fell within the chromosomal regions associated with the significant peaks in the all-family QTL. We searched for matches between our candidate gene list and pigmentation loci using previously curated and published pigmentation lists (Baxter et al., 2019; McKinnon et al., 2022). Second, we performed functional enrichment of Gene ontology terms associated with the candidate gene list to assess if any functional pathways were overly represented. We used the biomaRt package to extract gene position, gene IDs, HGNC symbols and associated gene ontology (GO) terms from the

stickleback genome (Durinck et al., 2009). The GO pathways associated with each gene ID of interest in our study was extracted and topGO was used to test for functional enrichment across our set of candidates (Alexa & Rahnenführer, 2023). To test for significant enrichment, a Fisher's exact test based on annotated gene counts was run that took into consideration GO hierarchy, and the algorithm was set to weight01. Significant GO terms were visualized using 'showSigOfNodes' and we identified which and how many genes in our candidate gene list were associated with these pathways.

Results

Pigmentation variation

The pigmentation phenotypes characterized in our F_2 mapping population of stained fish appeared to capture a biologically relevant pigment trait present in live wild caught fish (Figure 2). There was evidence of a significant negative correlation between melanophore density of stained fish and brightness at the fin junction measured from living fish (r = -0.41, p <0.0001). Thus, the "brighter" the operculum (i.e., the less dark), the lower the melanophore density. There was also a significantly positive correlation between lateral barring in living and stained fish (r= 0.71, p < 0.0001). The strength of the relationship between these variables varied amongst the populations for both lateral barring (0.63 to 0.36) and melanophore density (-0.26 to -0.54).

Within the benthic-limnetic F_2 hybrid individuals used for QTL mapping, we did not find any relationship between the two surveyed pigmentation traits (melanophore density and lateral

barring) ($r = 0.01$; $p > 0.05$). This suggests that these phenotypes are largely independent of each other. Across the F_1 mapping families there were statistically significant differences in melanophore density ($F = 6.79$; $p < 0.0001$) and lateral barring ($F = 9.45$; $p < 0.0001$). In general, families two and three exhibited greater melanophore density at the fin junction, while families two and four displayed more lateral barring (Figure 3).

QTL mapping

Melanophore density

When mapping melanophore density across all four F_1 families, there was a single significant QTL peak, which was located on chromosome 8 (Figure 4A, S6). Examination of the 1.5-LOD support interval placed the peak in a region encompassing ≈8 Mb, between markers ChVIII:7120492 and ChVIII:14925951. The alleles at this QTL had predominantly additive effects (Figure 4B), although when family four was analyzed independently it exhibited a non-additive effect (Figure 4C). Across families, this QTL explained ~5% of the total phenotypic variance. Within each family the variance explained ranged from 7.4 – 10.2% (Family 1 = 7.42%; Family 2 = 10.21%; Family 3 = 7.85%; Family 4 = 9.03%). QTL mapping conducted *within* each F_1 family identified an additional peak in family 1 for melanophore density on chromosome 18 between markers ChXVIII:2652629 and ChXVIII:12506627 (Table 1) that explained 9% of the phenotypic variance. The total heritability of this trait was 0.28 when estimated across all families and markers.

Lateral Barring

In the all F_1 family QTL analysis for lateral barring, a significant candidate peak was identified on chromosome 21. Examination of the 1.5-LOD support interval places the peak in a region encompassing ≈7 Mb, between markers chrXXI:3061663 and chrXXI:10192631 (Figure 5A, S7). Similar to mapping for melanophore density, the effects were additive in the all-family analysis (Figure 5C). The overall percent variance explained was 4.26%, and phenotypic variance explained again differed among families ranging from 4.5 – 11% (Family 1 = 4.62%; Family 2 = 11.03%; Family 3 = 11.24%; Family 4 = 5.22%). One additional candidate on chromosome 16 was identified in the F_1 family 2 analysis (see Table 2). The total heritability of this trait was 0.35 across all families and markers.

Functional enrichment

Across both traits, we identified 1,099 loci associated within significant QTL intervals in both the all-family and within-family QTLs. Across the all-family crosses, there were 638 genes within the 1.5 LOD interval across both outlier chromosomal regions, and approximately 5% were previously identified pigmentation genes. Among the candidates resulting from our all-F_1 family map of melanophore density, we identified 350 candidate genes and 11 of these genes (~4%) were previously shown to be associated with pigmentation in other vertebrates. For lateral barring, we identified 288 candidates in the all-family cross and of these, 8 genes (~3%) were previously known vertebrate pigmentation loci.

To further investigate our set of candidates, we performed functional enrichment testing separately on candidate regions on chromosomes eight and twenty-one, for melanophore density and lateral barring, respectively. Using the lists of 140 and 119 annotated candidate genes we identified 22 significantly enriched pathways (Table 3). From the annotated chromosome 8 candidates, there were 8 enriched pathways: five involved in catalytic activity, one in transporter activity, one in binding, and the last in molecular function regulation (S8). Among the chromosome 21 candidates, there were 14 pathways significantly enriched: three involved in binding and the rest involved with catalytic activity (S9). Within these enriched pathways, three of the genes have been previously associated with pigmentation pathways (Table 3).

Discussion and Conclusion

We investigated the genetic basis of two melanin pigmentation phenotypes, lateral barring and melanophore density, using a large sample of benthic-limnetic F_2 hybrid stickleback. QTL mapping was conducted across and within families; the resulting candidates were compared to known pigmentation genes and their functions were explored using GO term analysis. Using this approach, we found that the two pigmentation traits were uncorrelated and mapped to distinct genetic regions (Figure 4A and 5A), suggesting they are independent traits. Melanocyte density mapped to chromosome 8 (Figure 4A), and degree of lateral barring mapped to chromosome 21 (Figure 5A). A previous QTL study of marine-freshwater stickleback crosses found candidates for melanization of the gills and ventral flank map to the *kitlg* locus on chromosome 19 (Miller et al., 2007). Prior work examining the degree of lateral barring in marine-freshwater crosses identified candidate regions on chromosomes 1, 6, and 11 (Greenwood et al., 2011). This suggests that distinct genes may underly different components of melanism across the body and/or that the genetic architecture of lateral barring may differ

between marine-freshwater populations relative to benthic-limnetic populations. Alternatively, the distinct loci underlying lateral barring in marine-freshwater pairs could be due to a failure to detect small effects in the benthic-limnetic crosses. Our results indicate that the effects on the QTL were additive (Figures 4B and 5B), which is in line with previous findings (Miller et al., 2014). The identified loci are of relatively small effect, suggesting that these traits are likely polygenic.

Large effect loci have been identified for several key ecological traits in stickleback including lateral plate count (>76% variance explained), neuromast pattern (>39% variance explained) and pelvic spine length (>65% variance explained) (Colosimo et al., 2005; Erickson et al., 2016; Wark et al., 2012). Yet, small effect loci also contribute to these traits, and variance in other important stickleback traits, including other defense traits (e.g. dorsal spine length), trophic traits (e.g. gill raker number and length, tooth number), and body shape have been shown to have a highly polygenic architecture with many loci of relatively small effect contributing to phenotypic variation (Erickson et al., 2016; Miller et al., 2014; Peichel & Marques, 2017). Prior work on melanization and degree of barring found a combination of relatively small effect loci (6.6-11.7% variance explained) and moderate effect loci (~20% variance explained) (Greenwood et al., 2011; Greenwood et al., 2012). In contrast, a large effect locus, *kitlg,* explains >56% of the variance in gill melanic pigments in marine-freshwater (Miller et al., 2007). Variability in the complexity of the architecture of pigmentation has also been found in other taxa. For example, in *Peromyscus* mice and several lizard species*,* differences in pigmentary loss or gain has been attributed to a single mutation (Hoekstra et al., 2006; Nachman et al., 2003; Rosenblum et al., 2010), while in *Drosophila*, the degree of melanization is often associated with a suite of small effect genes (Dembeck et al., 2015).

Within a single species, differences in genetic background can impact the phenotype through epistatic interactions. For example, in beach mice, lighter coloration associated with one gene (*mc1r*) is not apparent unless another gene (*asip*) also increases its expression (Steiner et al., 2008). The phenotypic and genetic effects of pigmentation loci will thus vary among and between populations and species (Hubbard et al., 2010; Manceau et al., 2010). Our results indicate variation between families in their expressed phenotypes, effect sizes, and dominance effects (Figure 3, 5C), which could be due to epistasis. A similar pattern of family level variation was detected previously when mapping skeletal traits in benthic-limnetic F_2 crosses (Rennison et al., 2019). The observed variation in mapped QTLs among F_1 families could result from the presence of different segregating variance present in the pure benthic and limnetic parents used for each F_1 cross. Alternatively, the variation in F_1 families may be a result of stochastic differences in power of detection of these relatively small effect loci. With only 100 individuals per family, loci near the significance cut off could fall just above the threshold in one family and below in another. Differences in the fraction of missing data across individuals for each family could also contribute to the pattern of variable detection. Unfortunately, due to the absence of inter F_1 family crosses and the relatively small sample sizes of the individual families we did not have the power or experimental framework to investigate these potential epistatic effects in this experiment.

From the candidate QTL regions for these two pigmentation traits, several new candidate pigmentation genes were identified for benthic and limnetic stickleback (S6). Three of the candidate loci (*sulf1*, *bco1*, *tyms*) were associated with functionally enriched pathways (Table 3). Of these, *bco1* has been previously associated with fish carotenoid pigmentation, including in threespine stickleback (Huang et al., 2021; McKinnon et al., 2022). Another candidate, *tyms*, is

389 known to lead to abnormal pigmentary patterns in zebrafish (Amsterdam et al., 2004; *Phenotype*
390 *Annotation (1994-2006)*, 2006). While all three of these genes are associated with pigmentation
391 phenotypes in other vertebrates, only one is associated with other stickleback pigmentation
392 phenotypes. Of the genes found proximate to our QTL peaks, >500 had no prior known role in
393 pigmentation and only 30 (~5.5%) were functionally enriched. Thus, our survey expands this
394 candidate list of potential loci underlying pigmentation evolution.
395 This study demonstrates that quantification/characterization of melanic pigmentation in
396 stained stickleback provides a likely functionally relevant estimation of melanic traits in living
397 fish. Previous pigmentation work on stickleback has been largely limited to phenotyping
398 conducted using photos from living fish, specimens phenotyped immediately following
399 euthanasia, or surveys of internal structures (Greenwood et al., 2011; Malek et al., 2012;
400 McKinnon et al., 2022; Yong et al., 2015). Our finding that pigmentation phenotypes collected
401 from preserved and stained specimens produce biologically meaningful data opens up additional
402 opportunities to study pigmentation using museum collections or in instances where live
403 photographs would be difficult to collect. Stickleback pigmentation genetics remains
404 understudied relative to other traits (Reid et al., 2021), and fish pigmentation genetics is
405 generally understudied relative to other vertebrates (Elkin et al., 2022). This is likely due in part
406 to pigmentation being more challenging to quantify in fish than in other vertebrates. For
407 example, while mammals have only one type of chromatophore, fish have six different kinds
408 (black melanophores, yellow-orange xanthophores, red erythrophores, light-reflecting
409 iridophores, white leucophores, blue cyanophores) (Cal et al., 2017; Kelsh, 2004). Many
410 chromatophores exhibit plasticity to environmental conditions (e.g., red erythrophores influenced
411 by carotenoid availability in the diet (Pike et al., 2011). However, the extent to which pigment

phenotypes can change depends on the concentrations of melanosomes (Logan et al., 2006). As such, melanic traits may be more static and thus more easily phenotyped. As the list of pigmentation QTLs grows for threespine stickleback—a model in evolutionary biology—it can aid us in understanding the predictability of phenotypic and genotypic evolution and the origins of adaptive genetic variation.

Acknowledgements

The authors wish to thank Vishwa Pandya and John Villalpando for assistance with phenotypic data collection.

Author Contributions

DJR conceived the study, and ET developed the phenotyping protocols to carry out the work. DJR performed the genotyping and ET performed the QTL mapping. DJR and ET interpreted the results, contributed to writing, and editing of the final version of the manuscript.

Competing Interests

The authors declare no competing financial interests.

Data Archiving

Underlying data and code are archived on GitHub:
https://github.com/djrennison/Heredity_pigment

References

Alexa, A., & Rahnenführer, J. (2023). Gene set enrichment analysis with topGO. *Bioconductor Improv* 27, 1-26.

Amsterdam, A., Nissen, R. M., Sun, Z., Swindell, E. C., Farrington, S., & Hopkins, N. (2004). Identification of 315 genes essential for early zebrafish development. *Proceedings of the National Academy of Sciences of the United States of America*, *101*(35), 12792–12797.

Anderson, T. M., vonHoldt, B. M., Candille, S. I., Musiani, M., Greco, C., Stahler, D. R., et al. (2009). Molecular and evolutionary history of melanism in North American gray wolves. *Science*, *323*(5919), 1339–1343.

Arnegard, M. E., McGee, M. D., Matthews, B., Marchinko, K. B., Conte, G. L., Kabir, S., et al. (2014). Genetics of ecological divergence during speciation. *Nature*, *511*(7509), 307–311.

Barrett, R. D. H., Laurent, S., Mallarino, R., Pfeifer, S. P., Xu, C. C. Y., Foll, M., et al. (2019). Linking a mutation to survival in wild mice. *Science*, *363*(6426), 499–504.

Baxter, L. L., Watkins-Chow, D. E., Pavan, W. J., & Loftus, S. K. (2019). A curated gene list for expanding the horizons of pigmentation biology. *Pigment Cell & Melanoma Research*, *32*(3), 348–358.

Bell, M. A., & Foster, S. A. (Eds.). (1994). *The Evolutionary Biology of the Threespine Stickleback,*. Oxford University Press.

Bolder, A.M., Lohse, M., & Usadel, B. (2014). Trimmomatic: a flexible trimmer for Illumina sequence data. *Bioinformatics*, *30*, 2114-2120.

Bolnick, D. I., & Ballare, K. M. (2020). Resource diversity promotes among-individual diet variation, but not genomic diversity, in lake stickleback. *Ecology Letters*, *23*(3), 495–505.

Boughman, J. W. (2001). Divergent sexual selection enhances reproductive isolation in sticklebacks. *Nature*, *411*(6840), 944–948.

Broman, K. W., & Sen, S. (2009). *A guide to QTL mapping with R/qtl*. Springer Science & Business Media.

Cal, L., Suarez-Bregua, P., Cerdá-Reverter, J. M., Braasch, I., & Rotllant, J. (2017). Fish pigmentation and the melanocortin system. *Comparative Biochemistry and Physiology*, *211*, 26–33.

Clarke, J. M., & Schluter, D. (2011). Colour plasticity and background matching in a threespine stickleback species pair. *Biological Journal of the Linnean Society. 102*(4), 902–914.

Colosimo, P. F., Hosemann, K. E., Balabhadra, S., Villarreal, G., Jr, Dickson, M., Grimwood, J., et al. (2005). Widespread parallel evolution in sticklebacks by repeated fixation of Ectodysplasin alleles. *Science*, *307*(5717), 1928–1933.

Crawford, N. G., Kelly, D. E., Hansen, M. E. B., Beltrame, M. H., Fan, S., Bowman, S. L., et al. (2017). Loci associated with skin pigmentation identified in African populations. *Science*, *358*(6365), eaan8433.

Cuthill, I. C., Allen, W. L., Arbuckle, K., Caspers, B., Chaplin, G., Hauber, M. E., et al. (2017). The biology of color. *Science*, *357*(6350).

Dembeck, L. M., Huang, W., Magwire, M. M., Lawrence, F., Lyman, R. F., & Mackay, T. F. C. (2015). Genetic Architecture of Abdominal Pigmentation in Drosophila melanogaster. *PLoS Genetics*, *11*(5), e1005163.

DePristo, M.A., Banks, E., Poplin, R., Garimella, K.V., Maguire, J.R., Hartl, C., et al. (2011). A framework for variation discovery and genotyping using next-generation DNA sequencing data. *Nature Genetics, 43*, 491-498.

Durinck, S., Spellman, P. T., Birney, E., & Huber, W. (2009). Mapping identifiers for the integration of genomic datasets with the R/Bioconductor package biomaRt. *Nature Protocols*, *4*(8), 1184–1191.

Elkin, J., Martin, A., Courtier-Orgogozo, V., & Emília Santos, M. (2022). Meta-analysis of the genetic loci of pigment pattern evolution in vertebrates. In *bioRxiv* (p. 2022.01.01.474697).

Elshire, R. J., Glaubitz, J. C., Sun, Q., Poland, J. A., Kawamoto, K., Buckler, E. S., & Mitchell, S. E. (2011). A robust, simple genotyping-by-sequencing (GBS) approach for high diversity species. *PloS One*, *6*(5), e19379.

Erickson, P. A., Glazer, A. M., Killingbeck, E. E., Agoglia, R. M., Baek, J., Carsanaro, S. M., et al. (2016). Partially repeatable genetic basis of benthic adaptation in threespine sticklebacks. *Evolution; International Journal of Organic Evolution*, *70*(4), 887–902.

French, C. M., Ingram, T., & Bolnick, D. I. (2018). Geographical variation in colour of female threespine stickleback (*Gasterosteus aculeatus*). *PeerJ*, *6*, e4807.

Greenwood, A. K., Jones, F. C., Chan, Y. F., Brady, S. D., Absher, D. M., Grimwood, J., et al. (2011). The genetic basis of divergent pigment patterns in juvenile threespine sticklebacks. *Heredity*, *107*(2), 155–166.

Greenwood, Anna K., Cech, J. N., & Peichel, C. L. (2012). Molecular and developmental contributions to divergent pigment patterns in marine and freshwater sticklebacks. *Evolution & Development*, *14*(4), 351–362.

Gygax, M., Rentsch, A. K., Rudman, S. M., & Rennison, D. J. (2018). Differential predation alters pigmentation in threespine stickleback (*Gasterosteus aculeatus*). *Journal of Evolutionary Biology*, *31*(10), 1589–1598.

Hidalgo, M., Curantz, C., Quenech'Du, N., Neguer, J., Beck, S., Mohammad, A., & Manceau, M. (2022). A conserved molecular template underlies color pattern diversity in estrildid finches. *Science Advances*, *8*(35), eabm5800.

Hoekstra, H. E., Hirschmann, R. J., Bundey, R. A., Insel, P. A., & Crossland, J. P. (2006). A single amino acid mutation contributes to adaptive beach mouse color pattern. *Science*, *313*(5783), 101–104.

Huang, D., Lewis, V. M., Foster, T. N., Toomey, M. B., Corbo, J. C., & Parichy, D. M. (2021). Development and genetics of red coloration in the zebrafish relative Danio albolineatus. *ELife*, *10, e70253*.

Hubbard, J. K., Uy, J. A. C., Hauber, M. E., Hoekstra, H. E., & Safran, R. J. (2010). Vertebrate pigmentation: from underlying genes to adaptive function. *Trends in Genetics: TIG*, *26*(5), 231–239.

Jablonski, N. G., & Chaplin, G. (2017). The colours of humanity: the evolution of pigmentation in the human lineage. *Philosophical Transactions of the Royal Society of London. Series B, 372*(1724).

Jones, F. C., Grabherr, M. G., Chan, Y. F., Russell, P., Mauceli, E., Johnson, J., et al. (2012). The genomic basis of adaptive evolution in threespine sticklebacks. *Nature*, *484*(7392), 55–61.

Jones, M. R., Mills, L. S., Alves, P. C., Callahan, C. M., Alves, J. M., Lafferty, D. J. R., et al. (2018). Adaptive introgression underlies polymorphic seasonal camouflage in snowshoe hares. *Science*, *360*(6395), 1355–1358.

Kelsh, R. N. (2004). Genetics and evolution of pigment patterns in fish. *Pigment Cell Research*, *17*(4), 326–336.

Lamason, R. L., Mohideen, M.-A. P. K., Mest, J. R., Wong, A. C., Norton, H. L., Aros, M. C., et al. (2005). SLC24A5, a putative cation exchanger, affects pigmentation in zebrafish and humans. *Science*, *310*(5755), 1782–1786.

Lavin, P. A., & McPhail, J. D. (1986). Adaptive divergence of trophic phenotype among freshwater populations of the threespine stickleback (*Gasterosteus aculeatus*). *Canadian Journal of Fisheries and Aquatic Sciences. Journal Canadien Des Sciences Halieutiques et Aquatiques*, *43*(12), 2455–2463.

Li, H., & Durbin, R. (2009). Fast and accurate short read alignment with Burrows-Wheeler transform. *Bioinformatics*, *25*, 1754-1760.

Logan, D. W., Burn, S. F., & Jackson, I. J. (2006). Regulation of pigmentation in zebrafish melanophores. *Pigment Cell Research / Sponsored by the European Society for Pigment Cell Research and the International Pigment Cell Society*, *19*(3), 206–213.

Lopes, R. J., Johnson, J. D., Toomey, M. B., Ferreira, M. S., Araujo, P. M., Melo-Ferreira, J., et al. (2016). Genetic basis for red coloration in birds. *Current Biology: CB*, *26*(11), 1427–1434.

Lunter, G., & Goddson, M. (2011). STAMPY: a statistical algorithm for sensitive and fast mapping of Illumina sequence reads. *Genome Research*, *21*, 936-939.

Luo, M., Lu, G., Yin, H., Wang, L., Atuganile, M., & Dong, Z. (2021). Fish pigmentation and coloration: Molecular mechanisms and aquaculture perspectives. *Reviews in Aquaculture*, *13*(4), 2395–2412.

Lynn Lamoreux, M., Delmas, V., Larue, L., & Bennett, D. (2010). *The colors of mice: A model genetic network*. John Wiley & Sons.

Malek, T. B., Boughman, J. W., Dworkin, I., & Peichel, C. L. (2012). Admixture mapping of male nuptial colour and body shape in a recently formed hybrid population of threespine stickleback. *Molecular Ecology*, *21*(21), 5265–5279.

Manceau, M., Domingues, V. S., Linnen, C. R., Rosenblum, E. B., & Hoekstra, H. E. (2010). Convergence in pigmentation at multiple levels: mutations, genes and function. *Philosophical Transactions of the Royal Society of London. Series B*, *365*(1552), 2439–2450.

Martin, A., & Orgogozo, V. (2013). The loci of repeated evolution: A catalog of genetic hotspots of phenotypic variation. *Evolution; International Journal of Organic Evolution*, *67*(5), 1235–1250.

McKenna, A., Hanna, M., Banks, E., Sivachenko, A., Cibulskis, K., Kernystsky, A., et al. (2010) The Genome Analysis Toolkit: a MapReduce framework for analyzing next-generation DNA sequencing data. *Genome Research*, 20*,* 1297–1303.

McKinnon, J. S., Newsome, W. B., & Balakrishnan, C. N. (2022). Gene expression in male and female stickleback from populations with convergent and divergent throat coloration. *Ecology and Evolution*, *12*(5), e8860.

Miller, C. T., Beleza, S., Pollen, A. A., Schluter, D., Kittles, R. A., Shriver, M. D., & Kingsley, D. M. (2007). Cis-regulatory changes in Kit ligand expression and parallel evolution of pigmentation in sticklebacks and humans. *Cell*, *131*(6), 1179–1189.

Miller, C. T., Glazer, A. M., Summers, B. R., Blackman, B. K., Norman, A. R., Shapiro, M. D., et al. (2014). Modular skeletal evolution in sticklebacks is controlled by additive and clustered quantitative trait loci. *Genetics*, *197*(1), 405–420.

Nachman, M. W., Hoekstra, H. E., & D'Agostino, S. L. (2003). The genetic basis of adaptive melanism in pocket mice. *Proceedings of the National Academy of Sciences of the United States of America*, *100*(9), 5268–5273.

Orteu, A., & Jiggins, C. D. (2020). The genomics of coloration provides insights into adaptive evolution. *Nature Reviews. Genetics*, *21*(8), 461–475.

Ooijen, J.W.V., & Voorrips, R.E. (2001). JoinMap 3.0, Software for the calculation of genetic linkage maps. *Plant Research International*, Wagemingen.

Peichel, C. L., Nereng, K. S., Ohgi, K. A., Cole, B. L., Colosimo, P. F., Buerkle, et al. (2001). The genetic architecture of divergence between threespine stickleback species. *Nature*, *414*(6866), 901–905.

Peichel, Catherine L., & Marques, D. A. (2017). The genetic and molecular architecture of phenotypic diversity in sticklebacks. *Philosophical Transactions of the Royal Society of London. Series B, Biological Sciences*, *372*(1713), 20150486.

Pike, T. W., Bjerkeng, B., Blount, J. D., Lindström, J., & Metcalfe, N. B. (2011). How integument colour reflects its carotenoid content: A stickleback's perspective. *Functional Ecology*, *25*(1), 297–304.

Protas, M. E., & Patel, N. H. (2008). Evolution of coloration patterns. *Annual Review of Cell and Developmental Biology*, *24*, 425–446.

Quillen, E. E., Norton, H. L., Parra, E. J., Lona-Durazo, F., Ang, K. C., Illiescu, F. M., et al. (2019). Shades of complexity: New perspectives on the evolution and genetic architecture of human skin. *American Journal of Physical Anthropology*, *168 Suppl 67*, 4–26.

Reid, K., Bell, M. A., & Veeramah, K. R. (2021). Threespine stickleback: A model system for evolutionary genomics. *Annual Review of Genomics and Human Genetics*, *22*, 357–383.

Rennison, D. J., Owens, G. L., Heckman, N., Schluter, D., & Veen, T. (2016). Rapid adaptive evolution of colour vision in the threespine stickleback radiation. *Proceedings. of The Royal Society B.*, *283*(1830), 20160242.

Rennison, D. J., Rudman, S. M., & Schluter, D. (2019). Genetics of adaptation: Experimental test of a biotic mechanism driving divergence in traits and genes. *Evolution Letters*, *3*(5), 513–520.

Roesti, M., Kueng, B., Moser, D., & Berner, D. (2015). The genomics of ecological vicariance in threespine stickleback fish. *Nature Communications*, *6*, 8767.

Rosenblum, E. B., Römpler, H., Schöneberg, T., & Hoekstra, H. E. (2010). Molecular and functional basis of phenotypic convergence in white lizards at White Sands. *Proceedings of the National Academy of Sciences of the United States of America*, *107*(5), 2113–2117.

Saenko, S. V., Lamichhaney, S., Barrio, A. M., Rafati, N., Andersson, L., & Milinkovitch, M. C. (2015). Amelanism in the corn snake is associated with the insertion of an LTR-retrotransposon in the OCA2 gene. *Scientific Reports*, *5*(1), 1–9.

Schluter, D., & McPhail, J. D. (1992). Ecological character displacement and speciation in sticklebacks. *The American Naturalist*, *140*(1), 85–108.

Steiner, C. C., Römpler, H., Boettger, L. M., Schöneberg, T., & Hoekstra, H. E. (2008). The genetic basis of phenotypic convergence in beach mice: Similar pigment patterns but different genes. *Molecular Biology and Evolution*, *26*(1), 35–45.

Stevens, M., Párraga, A., Cuthill, I.C., Partridge, J.C., & Troscianko T.S. (2007). Using digital photography to study animal coloration. *Biological Journal of the Linnean Societ,* 90(2), 211–237.

Tapanes, E., Lasisi, T., Kamilar, J.M., Bradley, B.J. (2022). Genomics and cellular biology of the primate pigmentation: lessons from other taxa. *Program of the 91st Annual Meeting of the American Association of Biological Anthropologists*, 1–209.

Vamosi, S. M., & Schluter, D. (2004). Character shifts in the defensive armor of sympatric sticklebacks. *Evolution; International Journal of Organic Evolution*, *58*(2), 376–385.

Wark, A. R., Mills, M. G., Dang, L.-H., Chan, Y. F., Jones, F. C., Brady, S. D., et al. (2012). Genetic architecture of variation in the lateral line sensory system of threespine sticklebacks. *G3* , *2*(9), 1047–1056.

Yong, L., Peichel, C. L., & McKinnon, J. S. (2015). Genetic architecture of conspicuous red ornaments in female threespine stickleback. *G3*, *6*(3), 579–588.

Tables:

Table 1. Highest peaks in each family associated with melanophore density

Sample	Chr	LOD	cM	Marker near peak	PVE
All Family	8.2	3.96*	33.99	chrVIII:11219937	5.18
Family 1	18	3.79*	44.99	chrXVIII:8361341	9.61

* indicates the peak passes the 5% significance threshold as determined by permutation.

Table 2. Highest peaks in each family associated with lateral barring.

Sample	Chr	LOD	cM	Marker near peak	PVE
All Family	21*	4.22	29.7	chrXXI:7342929	4.26
Family 2	16*	4.70	63.12	chrXVI:563523	19.45

* indicates the peak passes the 5% significance threshold determined through permutation.

609 **Table 3.** Significantly enriched pathways and genes associated with each chromosome

Pathway name	GO	Sig.	Expected	Fis	Genes
Chromosome 21- melanophore density					
Carboxypeptidase activity	0004788	2	0.16	0.011	*cpa6, cpb1*
Protein kinase activity	0003834	9	8.11	0.013	*mak, sgk3, cdk8, acad11, yes1, fastkd3, map3k22*
Beta-carotene 15,15'-dioxygenase activity	0004864	1	0.01	0.015	***bco1***
Thiamine diphosphokinase activity	0004333	1	0.01	0.015	*tpk1*
Thiamine triphosphate phosphatase activity	0050333	1	0.01	0.015	*thtpa*
Glycine-tRNA ligase activity	0004820	1	0.01	0.015	*gars1*
Nuclear thyroid hormone receptor binding	0001882	1	0.01	0.015	*ncoa2*
Thymidylate synthase activity	0046966	1	0.01	0.015	***tyms***
Protein dimerization activity	0004180	5	1.45	0.033	*msc, ncoa2, TCF24, bhlhe22, myca*
Deoxyribodipyrimidine photo-lyase activity	0004652	1	0.03	0.029	*cry-dash*
Methylated-DNA-[protein]-cysteine S-meth	0003779	1	0.04	0.044	*klhl40b*
Sulfuric ester hydrolase activity	0008484	1	0.04	0.044	***sulf1***
Hydroxymethylglutaryl-CoA reductase	0004420	1	0.04	0.044	*gdap1*
Chromosome 8 – lateral barring					
Furmarate hydratase activity	0004333	1	0.02	0.017	*fh*
Protein phosphatase inhibitor activity	0004864	1	0.02	0.017	*pp1r2*
Protein tyrosine kinase activity	0004713	17	9.27	0.021	*tie1, ror1, jak1, zap70, mknk2b, csnk1g2b, nek7, mast3b, jak3, EPHB3, obscna, matk, abl2,*
Galactosyltransferase activity	0008378	2	0.30	0.035	*b3gnt3.4, b3gnt7*
Thiol oxidase activity	0016972	1	0.03	0.035	*lhx4*
Coproporphyrinogen oxidase activity	0004109	1	0.03	0.035	*cpox*
Lipid transporter activity	0005319	1	0.05	0.051	*vtg3*
Histone binding	0042393	1	0.05	0.051	*uhrf1*

610 Key: Genes with known pigmentation associations in **bold**
611

612 **Figure Captions:**

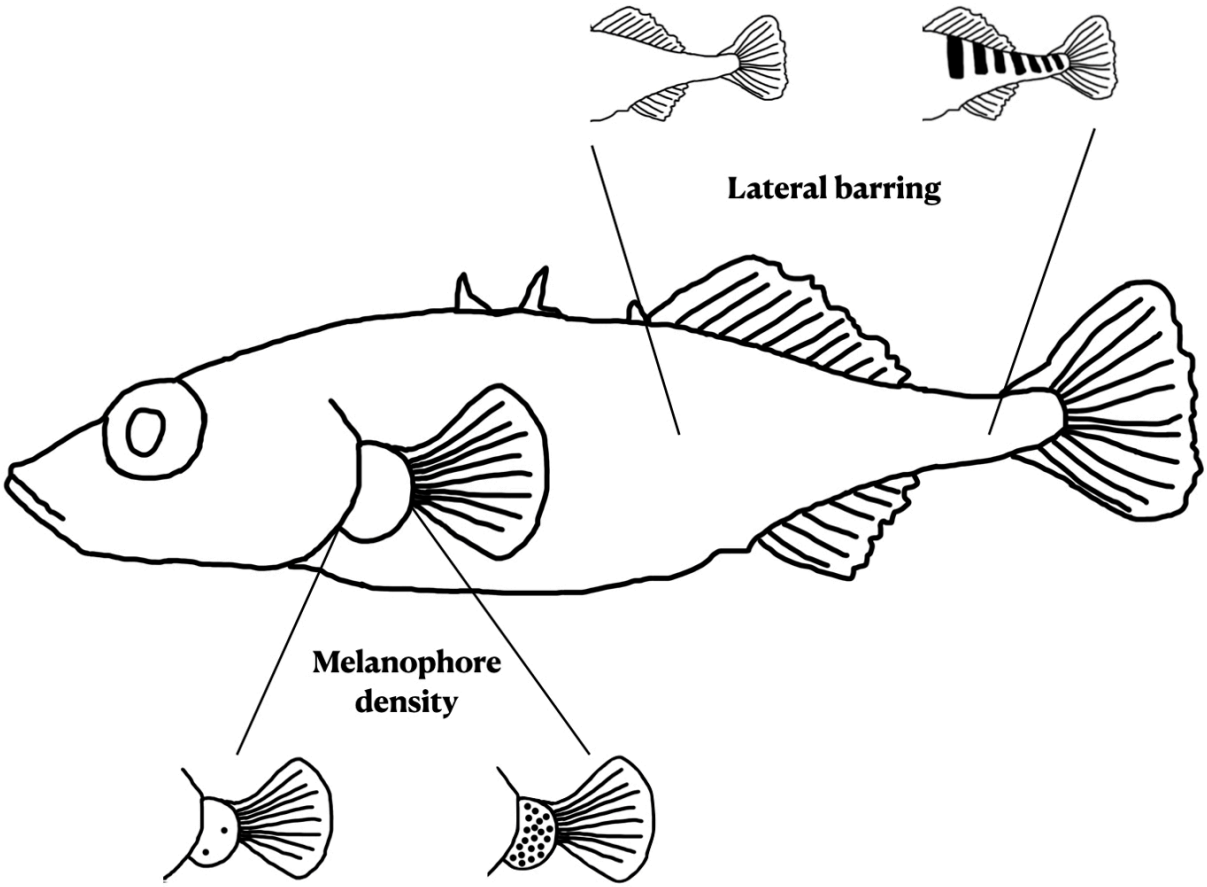

613
614 **Figure 1.** Stickleback phenotypes scored in this study: melanophore density of the fin junction

615 and the degree of lateral barring along the flank.

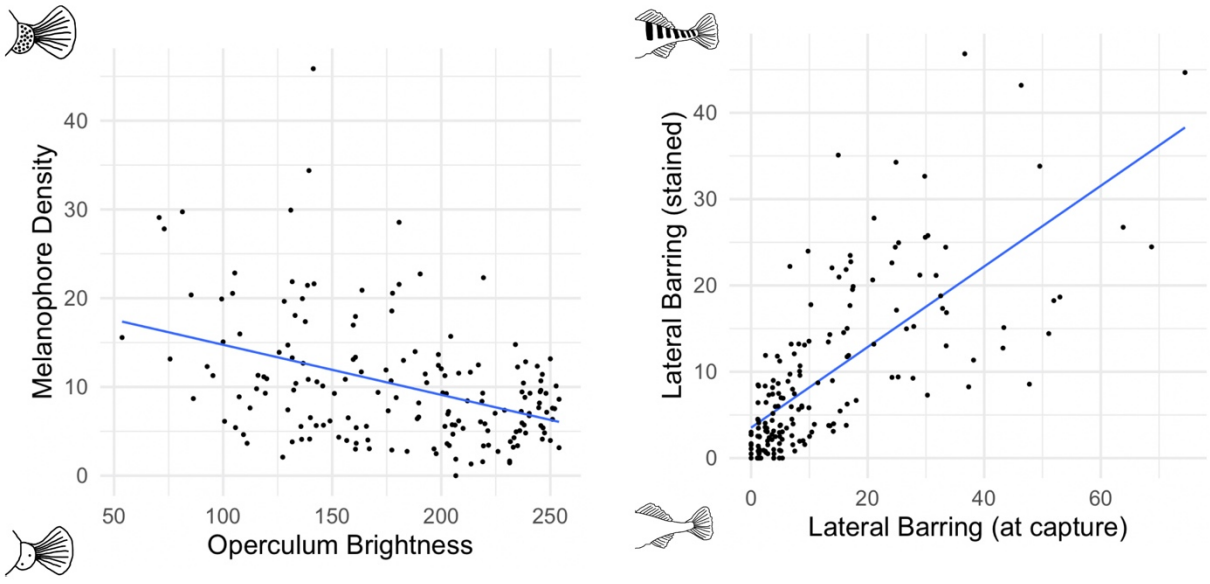

616

Figure 2. Pigmentation phenotypes in stained stickleback as they relate to pigmentation in non-stained living fish

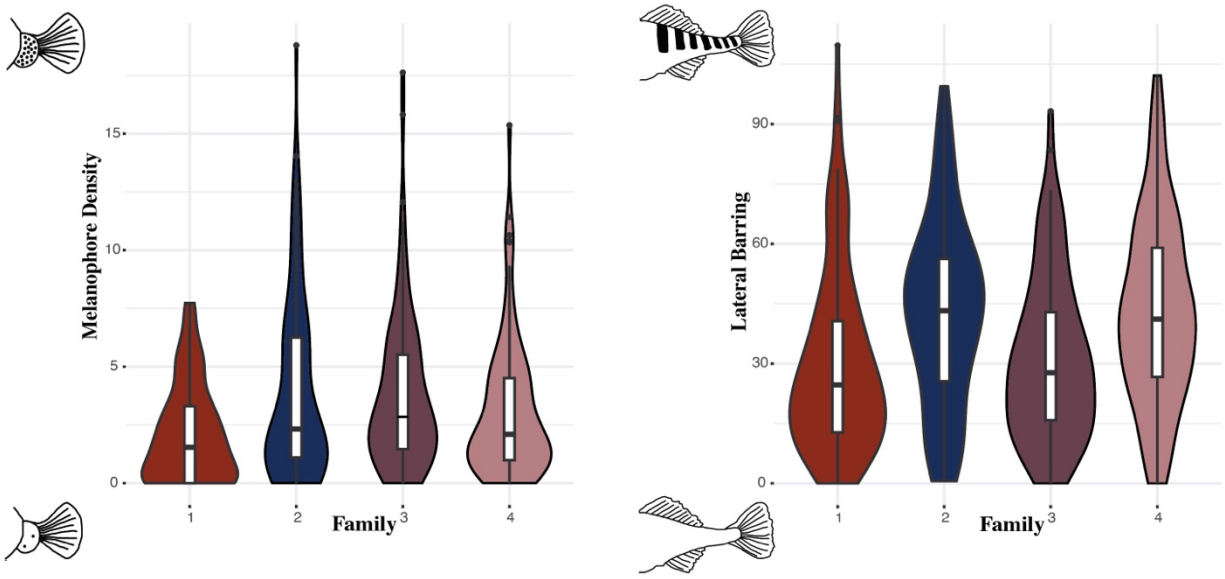

Figure 3. Distribution of melanophore density (number of visible melanocytes on the fin junction) and lateral barring (difference in light and dark patches on the ventral flank) across F_1 families of benthic-limnetic hybrids used for QTL mapping.

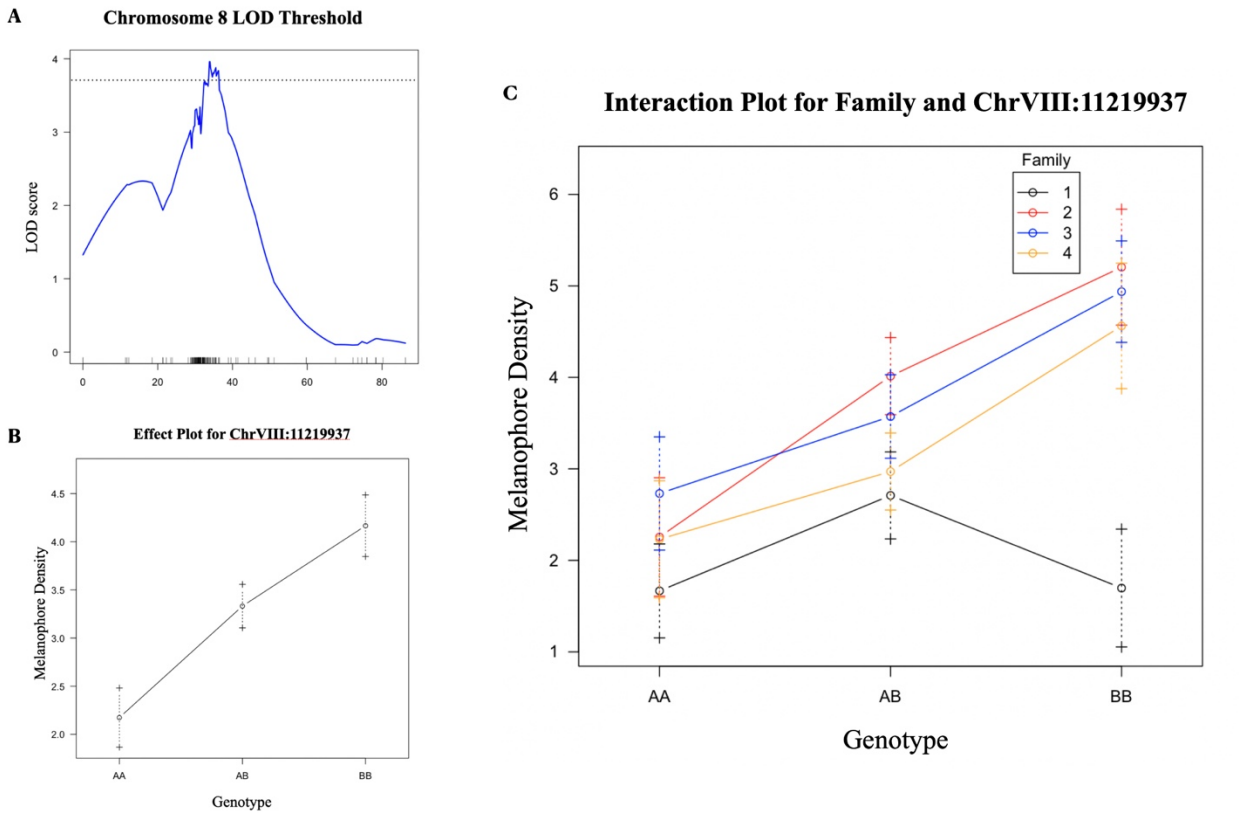

Figure 4. QTL mapping for melanophore density (1) LOD plot for chromosome eight candidate in the all-family analysis, (B) effect plot for chromosome eight candidate peak, and (C) interaction plot across the four F_1 families.

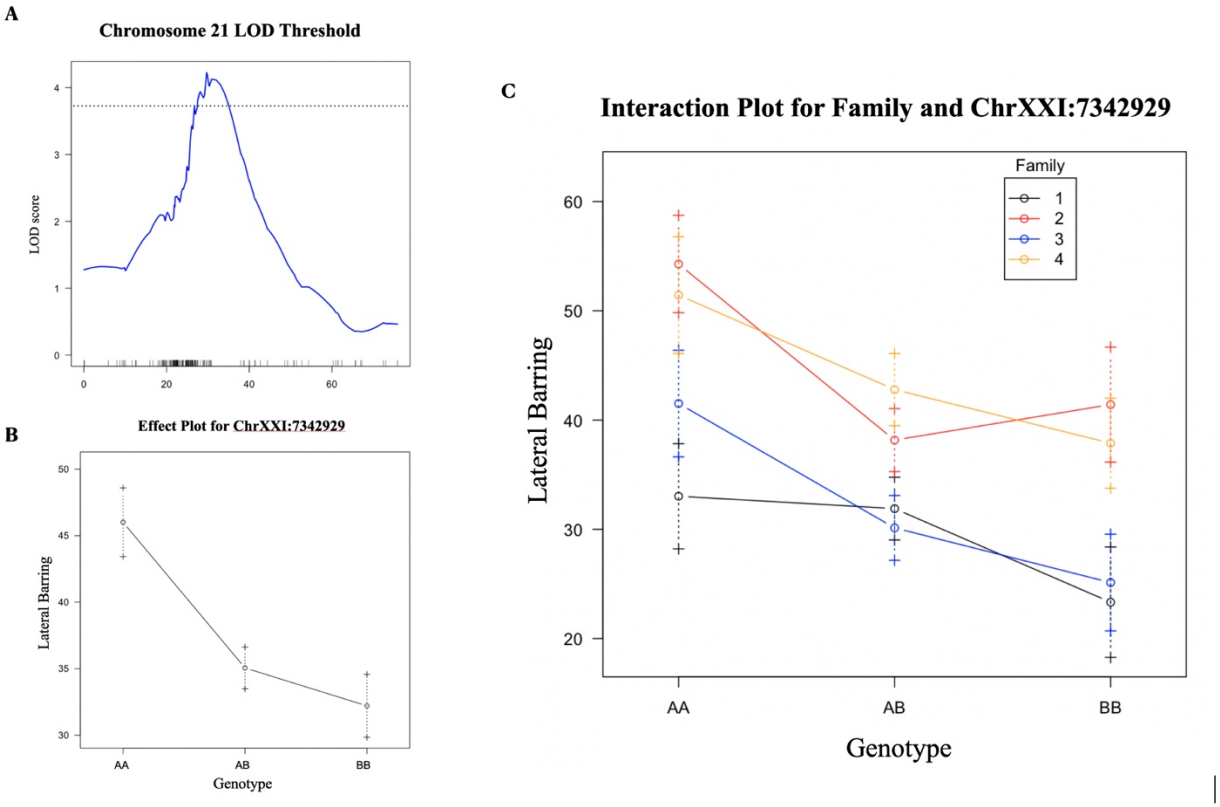

628
629 **Figure 5.** QTL mapping of Lateral barring (1) LOD plot for candidate on chromosomes twenty-
630 one in the all-family analysis, (B) effect plot for chromosome twenty-one candidate peak, and
631 (C) interaction plot across the four families.

632
633
634